arXiv:1510.01792v1 [physics.optics] 7 Oct 2015

Modeling of Space-Time Focusing of Localized Nondiffracting Pulses

Michel Zamboni-Rached[1,2] and Ioannis M. Besieris[3]

October 8, 2015

[1]University of Campinas, Campinas, SP, Brazil.

[2]Department of Electrical and Computer Engineering at the University of Toronto, Toronto, ON, Canada

[3]The Bradley Department of Electrical and Computer Engineering, Virginia Polytechnic Institute and State University, Blacksburg VA 24060, USA

Abstract

In this paper we develop a method capable of modeling the space-time focusing of nondiffracting pulses. The new pulses can possess arbitrary peak velocities and, in addition to being resistant to diffraction, can have their peak intensities and focusing positions chosen *a priori*. More specifically, we can choose multiple locations (spatial ranges) of space/time focalization; also, the pulse intensities can be chosen in advance. The pulsed wave solutions presented here can have very interesting applications in many different fields, such as free-space optical communications, remote sensing, medical apparatus, etc.

1 Introduction

It is well known that the scalar wave equation, in particular, and more generally Maxwell's equations have very interesting classes of solutions named Nondiffracting Waves [1–10], also called Localized Waves. These beams and pulses are immune to diffraction effects but have the drawback of containing infinite energy. This problem, however, can be solved [4, 6, 11–13] and the finite-energy versions of the ideal nondiffracting waves (INWs) can resist the diffraction effects for long (finite) distances when compared to the ordinary waves.

In this paper, we take a step forward in the theory of the nondiffracting pulses by introducing a new method that enables us to perform a space/time modelling on them. In other words, we can construct new nondiffracting localized pulse solutions in such a way that we can choose where and how intense their peaks will be within a longitudinal spatial range $0 \leq z \leq L$. This is not just an ordinary focusing method [14–16], where there is just one point of focalization; actually, it is a much more powerful method because it allows the choice of multiple locations (spatial ranges) of space/time focalization where the pulse intensities also can be chosen *a priori*.

Such modeling of the space/time evolution of ideal localized nondiffracting pulses with subluminal, luminal or superluminal peak velocities is made through a suitable and discrete superposition of ideal standard nondiffracting pulses. The new resulting waves can possess potential applications in many different fields, such as free-space optical communications, remote sensing, medical apparatus, etc.

In Section 2 we present important results related to ideal nondiffracting pulses with azimuthal symmetry, with the bidirectional and unidirectional decomposition approaches playing important roles. Section

3 is devoted to the modeling of the space-time focusing of localized nondiffracting pulses and examples are presented to confirm the efficiency of the method. Section 4 is devoted to the conclusions.

2 Important points related to the ideal (standard) nondiffracting pulses

In this section we present several important points regarding the ideal nondiffracting pulses, stressing the importance of the bidirectional and unidirectional decomposition methods used to deriving closed analytical solutions describing such waves. Here, we do not enter into mathematical details and demonstrations, as this subject has already been very well developed in a series of papers [6, 11–13].

Considering only propagating waves and azimuthal symmetry, the general solution to the homogeneous scalar wave equation, $\Box\psi = 0$ (with $\Box$ being the d'Alembertian), can be written in cylindrical coordinates as:

$$\psi(\rho,z,t) \;=\; \int_{-\infty}^{\infty} d\omega \int_{-\infty}^{\infty} dk_z \int_{0}^{\infty} k_\rho \, dk_\rho \, A'(k_\rho,k_z,\omega)\, \delta\left(k_\rho^2 - \left(\frac{\omega^2}{c^2} - k_z^2\right)\right) J_0(k_\rho\rho) e^{ik_z z} e^{-i\omega t} \tag{1}$$

with $A'(k_\rho,k_z,\omega)$ being an arbitrary function and $\delta(.)$ the Dirac delta function. The integral solution (1) is nothing but a superposition of zero-order Bessel beams involving the angular frequency (ω) and the transverse (k_ρ) and longitudinal (k_z) wave numbers.

It is well known [6, 11–13] that an ideal nondiffracting pulse with peak velocity $0 \leq V \leq \infty$ can be obtained when the spectrum $A'(k_\rho,k_z,\omega)$ forces a coupling of the type $\omega = Vk_z + b$, with b a constant, between the angular frequency and the longitudinal wave number. Such a coupling, and the solutions resulting from it, can be much more easily obtained when the bidirectional or unidirectional decompositions [6, 11–13] are adopted. These are characterized by changes from the spatial (z) and time (t) coordinates to the new ones, ζ and η, given by

$$\begin{cases} \zeta = z - Vt \\ \\ \eta = z + ut \end{cases} \tag{2}$$

with $V > 0$ and $\forall u \neq -V$. The transformation (2) is called bidirectional decomposition when $u > 0$, and unidirectional decomposition when $u \leq 0$.

In the new coordinates, the integral solution (1), after an integration on k_ρ, can be written as:

$$\psi(\rho,\zeta,\eta) \;=\; \int_{\alpha_{min}}^{\alpha_{max}} d\alpha \int_{\beta_{min}}^{\beta_{max}} d\beta S(\alpha,\beta) J_0(\rho\, s(\alpha,\beta))\, e^{-i\beta\eta} e^{i\alpha\zeta} \;, \tag{3}$$

where

$$s(\alpha,\beta) \;=\; \sqrt{\left(\frac{V^2}{c^2} - 1\right)\alpha^2 + \left(\frac{u^2}{c^2} - 1\right)\beta^2 + 2\left(\frac{uV}{c^2} + 1\right)\alpha\beta} \tag{4}$$

and $S(\alpha,\beta)$ is the spectral function, with the new spectral parameters α and β given by

$$\begin{cases} \alpha = \dfrac{1}{u+V}\left(\omega + uk_z\right) \\ \\ \beta = \dfrac{1}{u+V}\left(\omega - Vk_z\right) \end{cases} , \tag{5}$$

The limits of the integrals in Eq.(3) depend on the values of V and u and define the allowed values of α and β in order to avoid evanescent waves. In the plane (ω, k_z), these values correspond to the region between the straight lines $\omega = ck_z$ and $\omega = -ck_z$. To make easier the derivation of exact analytical solutions, we can choose a subdomain of the allowed values, considering, for instance, the first and fourth quadrants of the plane (ω, k_z).

Now, with the integral representation (1) it is quite simple to consider spectra that fix a relation of the type $\omega = Vk_z + b$ which, as we have said, yield ideal nondiffracting pulses. For this, with the new spectral parameters, we just need a new spectral function of the type

$$S(\alpha, \beta) \;=\; \delta(\beta - \beta_0) A(\alpha, \beta) \;, \tag{6}$$

with β_0 a constant. Due to the Dirac delta function $\delta(\beta - \beta_0)$ in the spectrum, the integral expression (3) becomes a superposition of zero-order Bessel beams with ω and k_z lying on the straight line* $\omega = Vk_z + (u + V)\beta_0$. The pulse peak velocity will be given by V and can be subluminal ($V < c$), luminal ($V = c$) or superluminal ($V > c$). The value of u in the decomposition (2) can be chosen to facilitate the analytical and exact integration of (3).

On the first and fourth quadrants of the plane (ω, k_z), Fig.(1) shows the semi-straight lines and the line-segment given by $\beta = \beta_0$ which define the different types of ideal nondiffracting pulses.

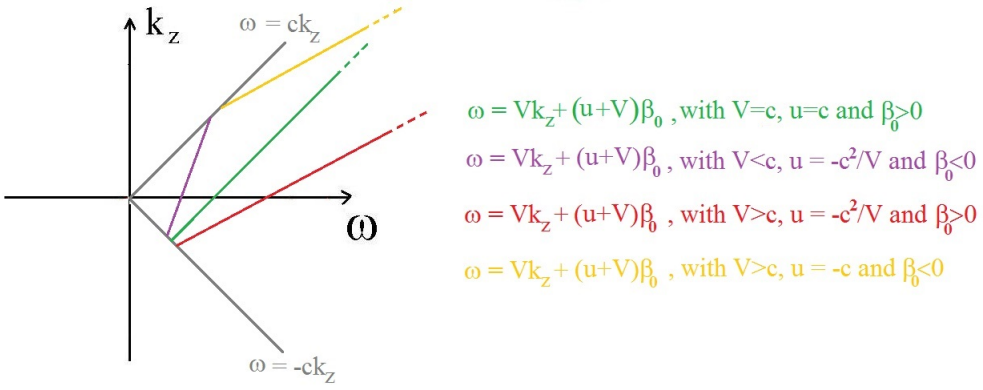

Figure 1: The semi-straight lines and the line segment given by $\beta = \beta_0 \rightarrow \omega = Vk_z + (u + V)\beta_0$ which define the different types of ideal nondiffracting pulses. The values chosen for u are those that make easier the exact integration of Eq.(3).

By using Eq.(6), with $\beta_{min} < \beta_0 < \beta_{max}$, in (3) we get

$$\psi(\rho, \zeta, \eta) \;=\; e^{-i\beta_0 \eta} \int_{\alpha_{min}}^{\alpha_{max}} d\alpha A(\alpha, \beta_0) J_0(\rho\, s(\alpha, \beta_0))\, e^{i\alpha\zeta} \;. \tag{7}$$

In general, the spectra $A(\alpha, \beta_0)$ used in the Localized Wave theory yield pulses centered on $\zeta = 0 \rightarrow z = Vt$. Below we list several important nondiffracting pulses obtained from Eq.(7).

- Subluminal MacKinnon-type pulse:

$$\psi(\rho, \zeta, \eta) \;=\; \mathcal{N}\, e^{-i\beta_0 \eta}\, \mathrm{sinc}\left(\frac{c}{V}|\beta_0|\sqrt{\gamma^{-2}\rho^2 - (a_1 + i\zeta)^2}\right) \;, \tag{8}$$

where $a_1 > 0$, $\gamma = (1 - V^2/c^2)^{-1/2}$ and $\mathcal{N} = -2a_1 c\beta_0 \exp(a_1 c\beta_0/V)/[V(1 - \exp(2a_1 c\beta_0/V))]$.

*This can be understood by noting that the Dirac delta function forces the condition $\beta = \beta_0 \rightarrow \omega = Vk_z + (u + V)\beta_0$

This pulse [11,17–20] is obtained from Eq.(7) considering $V < c$, $u = -c^2/V$, $\beta_0 < 0$, $\alpha_{min} = c\beta_0/V$, $\alpha_{max} = -c\beta_0/V$ and $A(\alpha, \beta_0) = -V\mathcal{N}/(2c\beta_0)\exp(a_1\alpha)$.

It is possible to show [20] that in order to minimize the contribution of the backward components to this solution it is necessary that $a_1 >> V/[|\beta_0(c+V)|]$. It is also possible to show that, with this condition on a_1, the central angular frequency of this pulse is $\omega_c \approx c^2(V/c+1)|\beta_0|/V$, with a frequency bandwidth $\Delta\omega \approx V/a_1$.

The modulus square of the Mackinnon pulse is undistorted during the propagation, with a spot size of radius $\Delta\rho_0 = \gamma\sqrt{(\pi V/|\beta_0|c)^2 + a_1^2}$.

- The Luminal Focus Wave Mode (FWM):

$$\psi(\rho, \zeta, \eta) \;=\; a_1 \frac{e^{-i\beta_0\eta}}{a_1 - i\zeta} \exp\left(-\frac{\beta_0\rho^2}{a_1 - i\zeta}\right) \tag{9}$$

This pulse [6] is obtained from Eq.(7) considering $V = c$, $u = c$, $\beta_0 > 0$, $\alpha_{min} = 0$, $\alpha_{max} = \infty$ and $A(\alpha, \beta_0) = a_1\exp(-a_1\alpha)$, with $a_1 > 0$ a constant.

It is possible to show [21, 22] that the central frequency of this pulse is $\omega_c = c\beta_0 + c/2a_1$, with a bandwidth $\Delta\omega \approx c/a_1$. It is also possible to show [6, 21, 22] that in order to minimize the contribution of the backward (wave) components of this solution (i.e., to make it causal) it is necessary that $a_1 << 1/\beta_0$, which implies that $\Delta\omega \approx 2\omega_c$. Such wideband frequency spectrum is a necessary condition to ensure the causality of the FWM pulse. This may give the wrong idea that luminal nondiffracting pulses must be ultrashort. Actually, although it is the case for the FWM solution, the existence of completely causal luminal nondiffracting pulses with arbitrary frequency bandwidths is quite possible and the only issue is that we do not know exact analytical solutions for these cases, which of course can be obtained through numerical simulations.

The modulus square of the FWM pulse is undistorted during the propagation, with a spot size of radius $\Delta\rho_0 = \sqrt{a_1/(2\beta_0)}$.

- The Superluminal Focus Wave Mode (SFWM):

$$\psi(\rho, \zeta, \eta) \;=\; \mathcal{N}\frac{e^{-i\beta_0\eta}}{\sqrt{\gamma'^{-2}\rho^2 + (a_1 - i\zeta)^2}} \exp\left(-\frac{c}{V}\beta_0\sqrt{\gamma'^{-2}\rho^2 + (a_1 - i\zeta)^2}\right), \tag{10}$$

where $a_1 > 0$, $\gamma' = (V^2/c^2 - 1)^{-1/2}$ and $\mathcal{N} = a_1\exp(a_1c\beta_0/V)$. This pulse [11–13] is obtained from Eq.(7) considering $V > c$, $u = -c^2/V$, $\beta_0 > 0$, $\alpha_{min} = c|\beta_0|/V$, $\alpha_{max} = \infty$ and $A(\alpha, \beta_0) = \mathcal{N}\exp(-a_1\alpha)$.

It is possible to show [6, 11, 12] that to minimize the contribution of the backward components to this solution it is necessary that $a_1 << V/[(V-c)\beta_0]$. It is also possible to show that the central frequency of this pulse is $\omega_c = (1 - c/V)c\beta_0 + V/(2a_1)$, with an angular frequency bandwidth $\Delta\omega = V/a_1$ which, due to the condition on a_1, can be approximated by $\Delta\omega \approx 2\omega_c$. The ultra wideband frequency spectrum also occurs here but, as in the luminal case, it is not a fundamental characteristic of superluminal nondiffracting pulses as we will see in the next case.

The modulus square of the SFWM pulse is undistorted during the propagation, with a spot size of radius $\Delta\rho_0 = \gamma'\sqrt{[a_1 + V/(2c\beta_0)]^2 - a_1^2}$.

- The Superluminal Focus Wave Mode totally free of backward components:

$$\psi(\rho,\zeta,\eta) \;=\; a_1 X e^{-i\beta_0\eta}\exp\left[-\frac{\beta_0}{\frac{V}{c}+1}\left(a_1 - i\zeta - X^{-1}\right)\right], \tag{11}$$

where $X=[\gamma'^{-2}\rho^2+(a_1-i\zeta)^2]^{-1/2}$ is the classical X-wave solution, $a_1>0$ and $\gamma'=(V^2/c^2-1)^{-1/2}$. This pulse [13] is obtained from Eq.(7) considering $V>c$, $u=-c$, $\beta_0<0$, $\alpha_{min}=0$, $\alpha_{max}=\infty$ and $A(\alpha,\beta_0)=a_1\exp(-a_1\alpha)$. It possesses a central frequency $\omega_c=c|\beta_0|+V/(2a_1)$, with an angular frequency bandwidth $\Delta\omega=V/a_1$. It is important to note that this pulse solution is totally free of backward components which is a great advantage. Due to this, it can possess any time width, not necessarily characterized by wide-frequency bandwidths as it is usually the case with other nondiffracting pulses of known analytical solutions.

The modulus square of this pulse is undistorted during the propagation, with a spot size of radius $\Delta\rho_0 \approx \gamma' a_1\sqrt{(V/c+1)^2/(4\beta_0^2 a_1^2)+(V/c+1)/(a_1|\beta_0|)}$ in the case $a_1|\beta_0|>(V/c+1)/(2\sqrt{2}-2)$, otherwise we have $\Delta\rho_0\approx\gamma' a_1$.

The intensity of all the pulses described above are undistorted for all time. Actually, this is the basic characteristic of all known ideal nondiffracting pulses (and beams) which, as we have already said, possess infinite energy. The latter drawback can be addressed by truncating [23–25] the ideal solutions[†] (finite aperture generation) or by concentrating the spectrum $A'(k_\rho,k_z,\omega)$ entering Eq.(1) in a region surrounding the straight line $\omega=Vk_z+b$ instead of collapsing it exactly over that line [6,11–13]. In both cases, the resulting waves attain finite energy and are resistant to the diffraction effects for long (but not infinite) distances.

In the next section we are going to take a step forward in the theory of the Localized Waves by introducing a new method that will enable us to model the space-time focusing of ideal nondiffracting pulses.

3 The method for modelling the space-time focusing of ideal nondiffracting pulses

In general, the peak of an ideal nondiffracting pulse with azimuthal symmetry, $\psi(\rho,\zeta,\eta)$, occurs at

$$\rho=0 \;\text{ and }\; \zeta=0 \;\;(\text{i.e., } z=Vt) \;\rightarrow \eta=\left(1+\frac{u}{V}\right)z\equiv\left(1+\frac{u}{V}\right)z_p\,, \tag{12}$$

where we have used Eq.(2) and called $z=z_p$, z_p being the peak's z-position. In this case, the pulse's peak based on Eq.(7) is described by

$$\psi(\rho=0,\zeta=0,\eta=(1+u/V)z_p) \;=\; \exp\left[-i\left(1+\frac{u}{V}\right)\beta_0 z_p\right]\int_{\alpha_{min}}^{\alpha_{max}} d\alpha A(\alpha,\beta_0) \tag{13}$$

Next, a new pulse solution, Ψ, will be constructed in such a manner that both the position of its peak, as well as the intensity of the peak, can be chosen within a longitudinal spatial range $0\le z\le L$. The new pulse is defined as a superposition of LW pulses like those in Eq.(7), with the same spectral function $A(\alpha,\beta_0)$ but with values of β different from β_0, in such a way that we can write for the new solution:

[†]In this case the resulting field is given by diffraction integrals, which rarely can be solved analytically

$$\Psi(\rho=0,\zeta=0,\eta=(1+u/V)z_p) \equiv \sum_{n=-N}^{N} B_n\, U_n \exp\left[-i\left(1+\frac{u}{V}\right)\beta_n z_p\right] \tag{14}$$

where $U_n = \int_{\alpha_{min}}^{\alpha_{max}} d\alpha A(\alpha,\beta_n)$, with the coefficients B_n and the values of β_n yet unknown.

If the choices

$$\beta_n = \frac{1}{1+u/V}\left(Q+\frac{2\pi}{L}n\right) \tag{15}$$

and

$$B_n = \frac{1}{L\,U_n}\int_0^L F(z_p) e^{i\frac{2\pi n}{L}z_p} dz_p \ , \tag{16}$$

are made, with Q and $F(z_p)$ a constant and an arbitrary function, respectively, the intensity of the expression in Eq.(14) within $0 \leq z_p \leq L$ will result in:

$$|\Psi(\rho=0,\zeta=0,\eta=(1+u/V)z_p)|^2 = |F(z_p)|^2 \tag{17}$$

and so we can chose, through the function $F(z_p)$, the locations and how intense the pulse's peak will appear.

The 3D *exact solution* is given by:

$$\Psi(\rho,\zeta,\eta) \ = \ \sum_{n=-N}^{N} B_n \psi_n(\rho,\zeta,\eta) \ , \tag{18}$$

where

$$\psi_n(\rho,\zeta,\eta) \ = \ e^{-i\beta_n\eta}\int_{\alpha_{min}}^{\alpha_{max}} A(\alpha,\beta_n) J_0(\rho\, s(\alpha,\beta_n))\, e^{i\alpha\zeta} \tag{19}$$

This approach is different from the ordinary space/time focusing methods, as those developed in [14–16], where there is just one point of focalization. It is a much more powerful method because, we repeat, it allows us to choose multiple locations (spatial ranges) of space/time focalization, where the pulse intensities also can be chosen *a priori*. This technique can be seen as a pulsed version of the Frozen Wave method [26–31] (originally developed for beams) and it can be implemented for subluminal, luminal and superluminal pulsed solutions. It is important to note that within all focal lines, the resulting pulses will be nondiffracting.

In general, the nondiffracting pulses ψ_n given in Eq.(19), and used in the new solution (18), have all their β_n with the same signal, positive or negative. Once we have chosen the values of β_0 [which in turn defines the value of Q via Eq.(15)] and L, this fact will imply a maximum value allowed for N, which restricts the number $2N+1$ of terms in the fundamental superposition (18). The maximum value of N can be obtained from Eq.(15), with the requirement that the signal of all β_n has to be equal to the signal for the chosen β_0.

It is not difficult to show that in any case the maximum value of N in (18) has to obey:

$$N \leq \frac{|1+u/V|}{2\pi}\, L\, |\beta_0| \tag{20}$$

With the method in hand, a natural question emerges: Which criteria should be used in choosing the values of the parameters β_0, which determines Q through Eq.(15), L and any other appearing within the spectral function $A(\alpha,\beta_n)$ in Eq.(19), which defines ψ_n?

First we have to say that any new solution $\Psi(\rho,\zeta,\eta)$, given by Eq.(18), will have several important characteristics associated to it, such as a central frequency, frequency bandwidth and the transverse spot size, which will be approximately similar to those presented by the central pulse, ψ_0, of the superposition (18). These characteristics of ψ_0 are described by equations involving the parameters β_0 and those occurring in $A(\alpha,\beta_0)$, which, therefore, can be determined once the desired characteristics mentioned above are chosen[‡].

The value of L cannot be evaluated in this way, but a good criterion is to choose it taking as reference the diffraction length, Z_{gauss} of a Gaussian pulse possessing the same spot size of the desired new pulse. Good choices for L would be those limited to values not much greater than hundred or thousand times the value of Z_{gauss}, otherwise we risk dealing with unrealistic situations in experimental apparatus sizes to generate the finite energy version of the pulse.

Having presented our method, we are going to illustrate it with a few examples, which will confirm its efficiency and simplicity.

It is important to notice that in the following examples some of the desired pulse's peak evolution patterns involve step functions, which are discontinuous. However, the resulting pulses will not present any discontinuity because they are given by a discrete and finite superposition of continuous pulsed solutions [see Eq.(18)]. Actually, what we are going to get are resulting pulses that approach the desired patterns, maintaining however the necessary properties of continuity and differentiability.

First example:

Here, we shall model the space-time focusing of a subluminal nondiffracting pulse. To do this, we are going to use the fundamental solution (18), with the ψ_n given by the subluminal MacKinnon solution in Eq.(8), with β_0 replaced with β_n.

In this case, we can set the parameters β_0 [which defines Q through Eq.(15] and a_1 according to the central frequency and frequency bandwidth of the resulting pulse, remembering that these characteristics are approximately similar to those of the central pulse ψ_0 of the superposition (18). In this case, ψ_0 is given by the Mackinnon-type solution, Eq.(8), whose characteristics cited above were presented in the previous section.

Considering a peak velocity $V = 0.999c$, with $u = -c^2/V$, a central angular frequency $\omega_c = 2.98 \times 10^{15}$rad/s and a frequency bandwidth $\Delta\omega \approx 10^{-2}\omega_c$, we can get $\beta_0 = -4.96 \times 10^6 \mathrm{m}^{-1}$ and $a_1 = 1.01 \times 10^{-5}$m. With this, the intensity spot radius for the resulting pulse can be estimated as being $\Delta\rho_0 \approx 0.226$mm. Concerning the value of L, which defines the range $0 \leq z_p \leq L$ within which the space-time modelling will be made, we note that an ordinary (Gaussian) pulse with the same spot size considered here would possess a diffraction length $Z_{diff} = 0.14$m so, according to our previous considerations, the value of L should not be many orders of magnitude greater than this value for avoiding unrealistic situations. Let us choose $L = 30Z_{diff} \approx 4.2$m.

For the function $F(z_p)$, whose modulus square will shape the positions and intensity of the resulting pulse's peak in the range $0 \leq z_p \leq L$, let us choose a ladder intensity pattern on the space interval $L/3 \leq z_p \leq 2L/3$, and zero outside it. More specifically, we wish that within $0 \leq z \leq L$ the pulse's peak intensity obeys $|\Psi(\rho = 0, \zeta = 0, \eta = (1 + u/V)z_p)|^2 = |F(z_p)|^2$, with

[‡]In general, just the central frequency and the frequency bandwidth or just the central frequency and the spot-size are necessary to determine the values of β_0 and other possible parameters occurring in $A(\alpha,\beta_0)$

$$F(z_p) \;=\; \begin{cases} 1 & \text{for} \quad l_1 < z_p < l_2 \\ \sqrt{2} & \text{for} \quad l_2 < z_p < l_3 \\ \sqrt{3} & \text{for} \quad l_3 < z_p < l_4 \\ 0 & \text{otherwise} \quad , \end{cases} \tag{21}$$

Here, $l_1 = L/3$, $l_2 = L/3 + \Delta l$, $l_3 = L/3 + 2\Delta l$ and $l_4 = L/3 + 3\Delta l$, with $\Delta l = L/9$.

The resulting pulse is given by Eq.(18) with the coefficients B_n given by Eq.(16) and ψ_n given by Eq.(8) through the replacement $\beta_0 \to \beta_n$, with β_n given by Eq.(15). Here, the maximum allowed value for N is 6,616, but we will use $N = 60$.

Figure 2 shows, within the range $0 \leq z_p \leq L$, the evolution of the actual pulse's peak intensity, $|\Psi(\rho = 0, \zeta = 0, \eta = (1 + u/V)z_p)|^2$, in doted line and the desired spatial evolution for it, $|F(z_p)|^2$, in continuous line. We can see a good agreement between them.

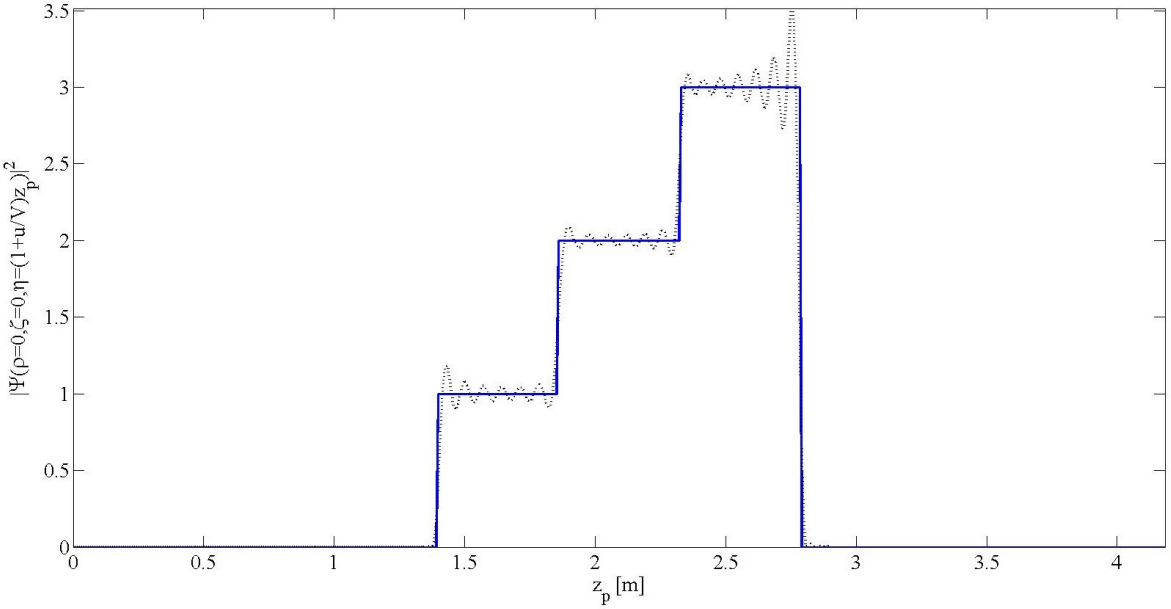

Figure 2: The peak intensity evolution, $|\Psi(\rho = 0, \zeta = 0, \eta = (1 + u/V)z_p)|^2$, of the resulting subluminal pulse is shown in doted line, while the desired peak intensity evolution for it, $|F(z_p)|^2$, is shown in continuous line. A good agreement between them is observed.

Even more interesting is Fig.(3), which shows the $3D$ pulse intensity – $|\Psi(\rho, \zeta, \eta)|^2$ – at nine different instants of time. More specifically, the first, second and third lines of the subfigures show the pulse evolution within the ranges $0 < z < L/3$, $L/3 < z < 2L/3$ and $2L/3 < z < L$, respectively. It is very clear that the resulting nondiffracting pulse possesses the desired space-time focusing characteristics.

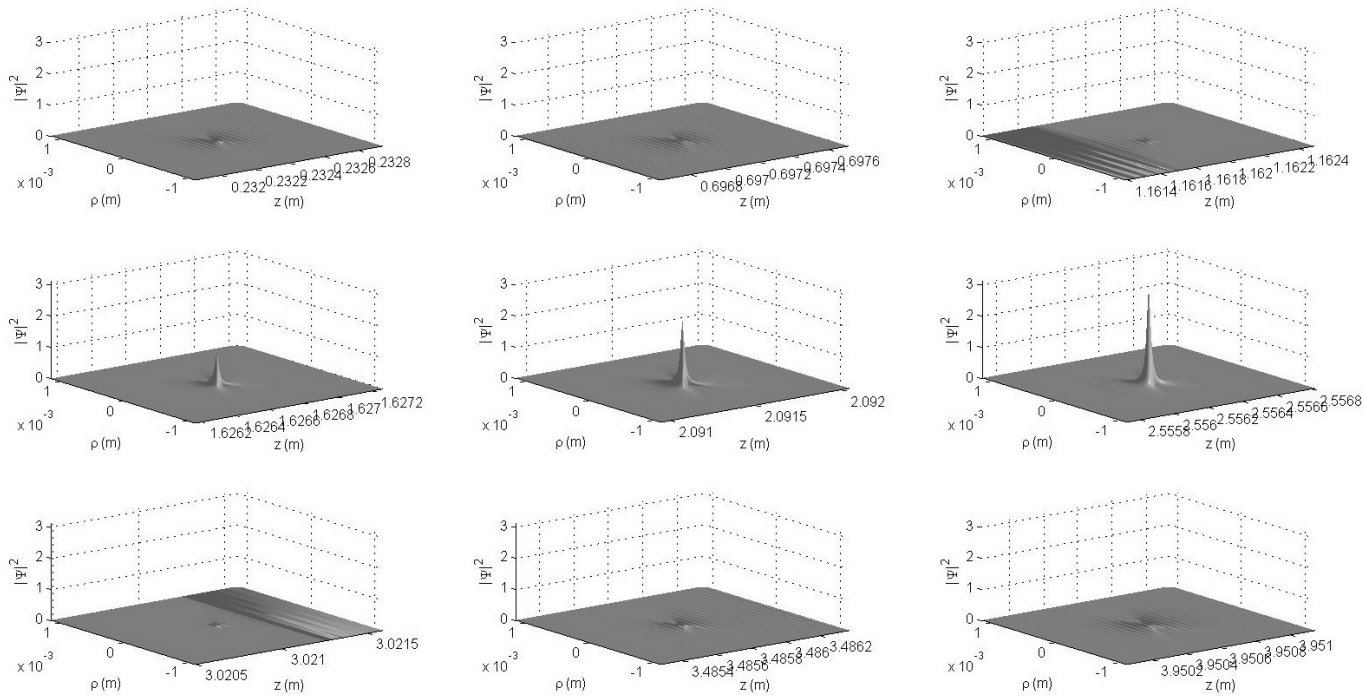

Figure 3: The $3D$ pulse intensity, $|\Psi(\rho,\zeta,\eta)|^2$, for the resulting subluminal pulse at nine different instants of time. The first, second and third lines of the subfigures show the pulse evolution within the ranges $0 < z < L/3$, $L/3 < z < 2L/3$ and $2L/3 < z < L$, respectively. We can see that the resulting nondiffracting pulse possesses the desired space-time focusing characteristics.

Second example:

Next, we are going to model the space-time focusing of a luminal nondiffracting pulse. For this, we will use our fundamental solution (18) with the ψ_n given by the luminal FWM solution, Eq.(9), with β_0 replaced by β_n. .

In this case, the parameters β_0 and a_1 are chosen according to the desired central frequency and transverse spot-size for the resulting pulse, these characteristics being approximately similar to those of the central pulse ψ_0 of the superposition (18). In this case, ψ_0 is given by the FWM solution, Eq.(9), of which the characteristics cited above were presented in the previous section.

Considering for the resulting pulse a peak velocity $V = c$, with $u = c$, a central angular frequency $\omega_c = 2.98 \times 10^{15}$rad/s and an intensity spot radius $\Delta\rho_0 = 10\mu$m, we obtain $\beta_0 = 2.518 \times 10^2 \mathrm{m}^{-1}$ and $a_1 = 5.036 \times 10^{-8}$m. In this case the frequency bandwidth is $\Delta\omega \approx 2\omega_c$. Furthermore, we choose $L = 0.516$m, which is 300 times greater than the diffraction length of a Gaussian pulse with the same spot size considered here.

Within the region $0 \leq z_p \leq L$ the pulse's peak intensity evolution obeys $|\Psi(\rho = 0, \zeta = 0, \eta = (1 + u/V)z_p)|^2 = |F(z_p)|^2$, with the choice

$$F(z_p) \;=\; \begin{cases} 1/\sqrt{2} & \text{for} \quad 0 < z_p < L/3 \\ 0 & \text{for} \quad L/3 < z_p < 2L/3 \\ 1 & \text{for} \quad 2L/3 < z_p < L \;, \end{cases} \tag{22}$$

The resulting pulse is given by Eq.(18) with the coefficients B_n given by Eq.(16) and ψ_n given by Eq.(9) through the replacement $\beta_0 \to \beta_n$, with β_n given by Eq.(15). Here, we use $N = 30$.

Figure 4 shows, within the range $0 \leq z_p \leq L$, a good agreement between the actual pulse's peak intensity evolution – $|\Psi(\rho = 0, \zeta = 0, \eta = (1 + u/V)z_p)|^2$ – (doted line) and the desired spatial evolution – $|F(z_p)|^2$ – for it (continuous line).

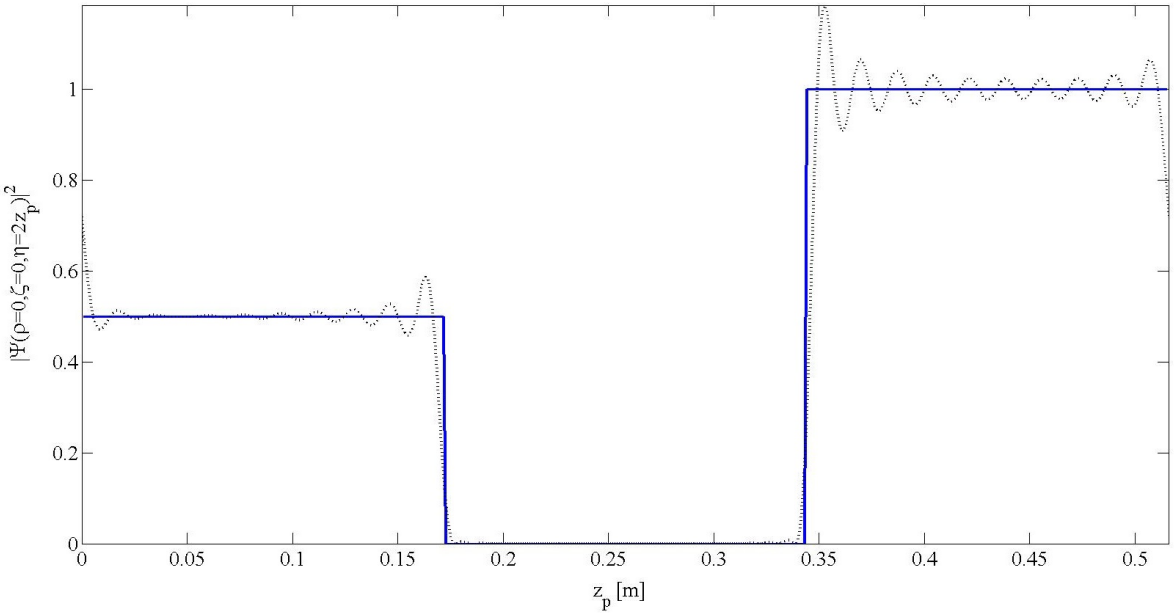

Figure 4: The peak intensity evolution, $|\Psi(\rho = 0, \zeta = 0, \eta = (1+u/V)z_p)|^2$, of the resulting luminal pulse is shown in doted line, while the desired peak intensity evolution for it, $|F(z_p)|^2$, is shown in continuous line. A good agreement between them is seen.

Figure (5) shows the $3D$ evolution of the pulse intensity – $|\Psi(\rho, \zeta, \eta)|^2$ – at nine different instants of time. The first, second and third lines of subfigures show the pulse evolution within the ranges $0 < z < L/3$, $L/3 < z < 2L/3$ and $2L/3 < z < L$, respectively. It is clear that the resulting nondiffracting pulse possesses the desired space-time focusing characteristics.

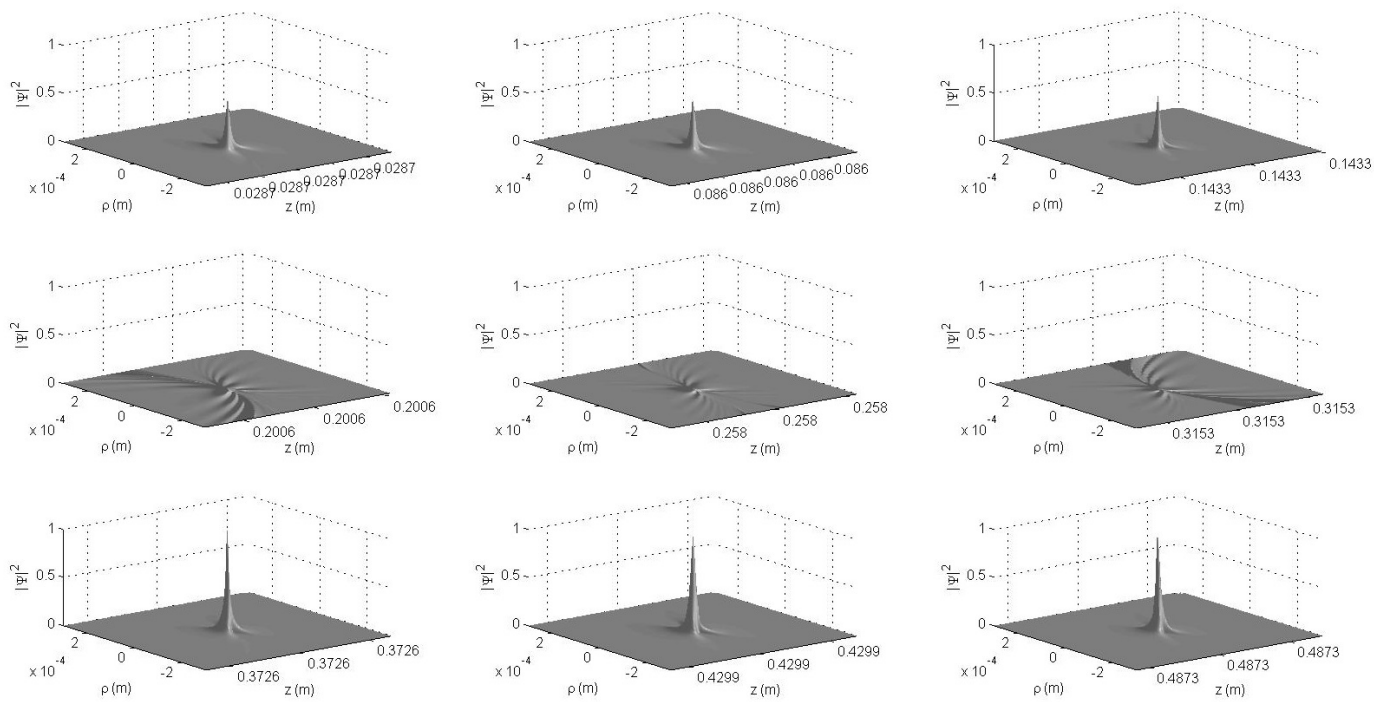

Figure 5: The $3D$ pulse intensity, $|\Psi(\rho,\zeta,\eta)|^2$, for the resulting luminal pulse at nine different instants of time. The first, second and third lines of the subfigures show the pulse evolution within the ranges $0 < z < L/3$, $L/3 < z < 2L/3$ and $2L/3 < z < L$, respectively. We can see that the resulting nondiffracting pulse possesses the desired space-time focusing characteristics.

Third example:

Finally, we shall model the space-time focusing of a superluminal nondiffracting pulse. Again, we use our fundamental solution (18), but now with the ψ_n given by the superluminal solution in Eq.(11) with β_0 replaced with β_n.

Considering a peak velocity $V = 1.0001c$, with $u = -c$, a central angular frequency $\omega_c = 2.98 \times 10^{15}$rad/s, a frequency bandwidth $\Delta\omega = \omega_c/10^3$, and following the same procedure as in the previous examples, but now considering ψ_0 as given by Eq.(11), we can get $\beta_0 = -9.9242 \times 10^6 \mathrm{m}^{-1}$ and $a_1 = 1.0072 \times 10^{-4}$m. In this case, the intensity spot radius for the resulting picosecond pulse can be estimated as being $\Delta\rho_0 \approx 0.32$mm. We also choose $L = 111.2$m, which is approximately 400 times greater than the diffraction length of a Gaussian pulse with the same spot size considered here.

For the space-time focusing modelling within $0 \leq z \leq L$, we wish the superluminal pulse's peak intensity $|\Psi(\rho = 0, \zeta = 0, \eta = (1 + u/V)z_p)|^2 = |F(z_p)|^2$ to behave as

$$F(z_p) \;=\; \begin{cases} 1 & \text{for} \quad l_1 < z_p < l_2 \\ \dfrac{\exp[(z - l_3)/(l_4 - l_3)] - 1}{e - 1} & \text{for} \quad l_3 < z_p < l_4 \\ 1 & \text{for} \quad l_5 < z_p < l_6 \;, \end{cases} \tag{23}$$

where $l_1 = 1.25\Delta l$, $l_2 = 1.75\Delta l$, $l_3 = 3\Delta l$, $l_4 = 5.5\Delta l$, $l_5 = 7.25\Delta l$ and $l_6 = 7.75\Delta l$, being $\Delta l = L/9$. This desired pattern for the evolution of the pulse's peak intensity is shown by Fig.(6) in continuous line.

The resulting pulse is given by Eq.(18) with the coefficients B_n given by Eq.(16) and ψ_n given by

Eq.(11) through the replacement $\beta_0 \to \beta_n$, with β_n given by Eq.(15). Here, we use $N = 70$.

Figure 6 shows, in doted line, the actual pulse's peak intensity profile along the axis, $|\Psi(\rho = 0, \zeta = 0, \eta = (1 + u/V)z_p)|^2$, which presents a good agreement with the desired pattern (continuous line).

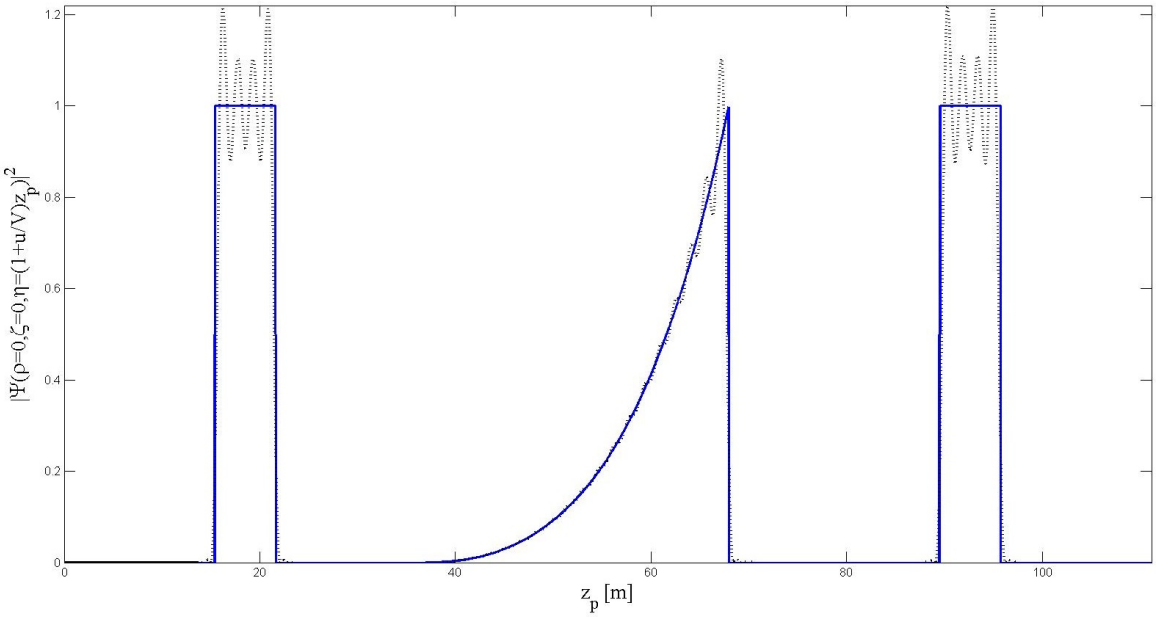

Figure 6: The peak intensity evolution, $|\Psi(\rho = 0, \zeta = 0, \eta = (1 + u/V)z_p)|^2$, of the resulting superluminal pulse is shown in doted line, while the desired peak intensity profile for it, $|F(z_p)|^2$, is shown in continuous line. A good agreement between them is observed.

Figure (7) shows the $3D$ evolution of the pulse intensity – $|\Psi(\rho, \zeta, \eta)|^2$ – at nine different instants of time. The first, second and third lines of subfigures show the pulse evolution within the ranges $0 < z < L/3$, $L/3 < z < 2L/3$ and $2L/3 < z < L$, respectively. Again, it is clear that the resulting nondiffracting pulse possesses the desired space-time focusing characteristics.

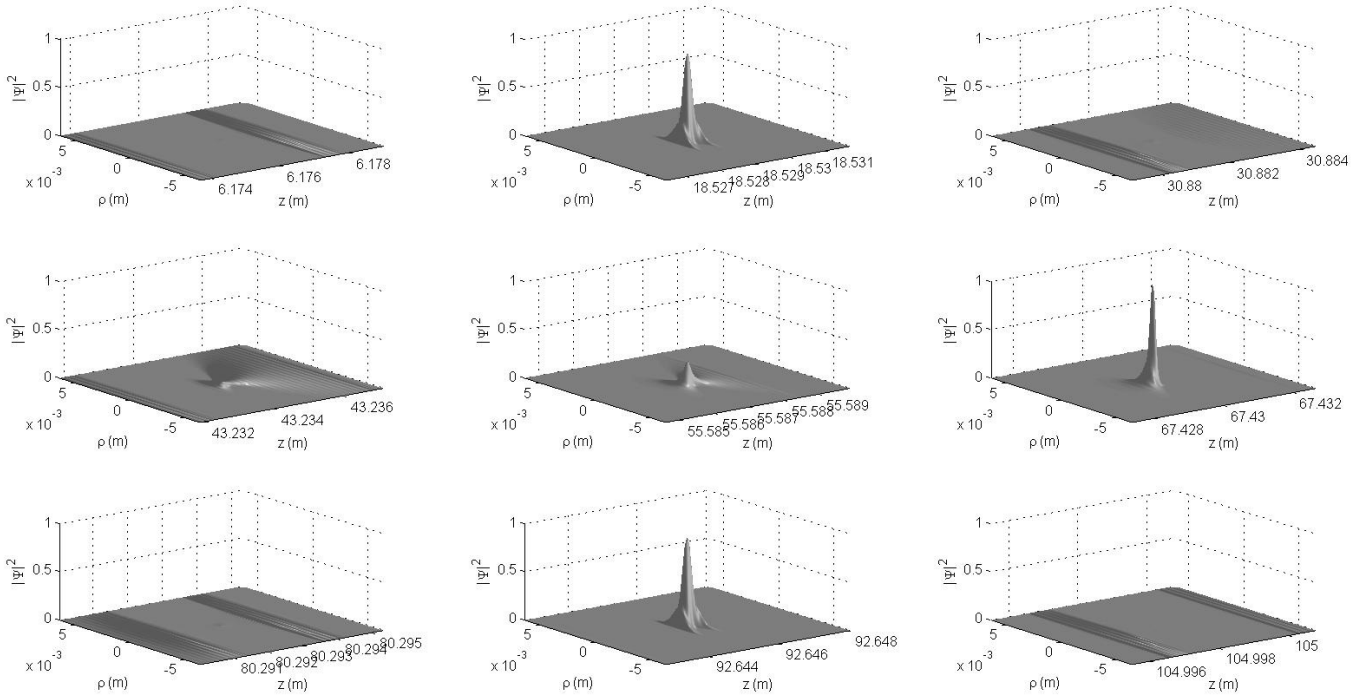

Figure 7: The $3D$ pulse intensity, $|\Psi(\rho,\zeta,\eta)|^2$, for the resulting superluminal pulse at nine different instants of time. The first, second and third lines of the subfigures show the pulse evolution within the ranges $0 < z < L/3$, $L/3 < z < 2L/3$ and $2L/3 < z < L$, respectively. We can see that the resulting nondiffracting pulse possesses the desired space-time focusing characteristics.

4 Conclusions

In this paper, a novel method has been presented that enables the modeling of space/time focusing of nondiffracting pulses. Specifically, it has been shown how to construct new localized pulse solutions in such a way that one can choose where and how intense their peaks will be within a longitudinal spatial range $0 \leq z \leq L$. This approach can be considered a step forward in the Localized Wave theory as it enables one to take advantage of the great potential of the nondiffracting wave pulses in a highly selective manner, by choosing *a priori* multiple locations (spatial ranges) of space/time focalization, with the pulse intensities also being chosen.

Space/time focusing modeling of ideal localized nondiffracting pulses with subluminal, luminal or superluminal peak velocities has been carried out by means of suitable superpositions of ideal standard nondiffracting pulses. The resulting new waves can have potential applications in many different fields, such as free-space optical communications, remote sensing, medical apparatus, etc.

The pulse solutions resulting from the space/time focusing method possess infinite energy content as they are obtained from discrete superpositions of ideal nondiffracting pulses. The finite energy version of our method will be presented elsewhere.

Acknowledgements

The authors thank Mo Mojahedi for valuable discussions and kind collaboration.

This work was supported by FAPESP (under grant 2013/26437-6); CNPq (under grants 312376/2013-

8).

References

[1] C.J.R.Sheppard, "Electromagnetic field in the focal region of wide-angular annular lens and mirror systems," *IEEE Journal on Microwaves, Optics and Acoustics*, Vol. 2, pp. 163-166 (1983).

[2] J. N. Brittingham, "Focus wave modes in homogeneous Maxwell's equations: transverse electric mode," J. Appl. Phys., Vol. 54, pp. 1179-1189 (1983).

[3] A. P. Kiselev, "Modulated Gaussian Beams," Radiophysics and Quantum Electronics, Vol.26, pp. 755-761 (1983).

[4] A. Sezginer, "A general formulation of focus wave modes," J. Appl. Phys., Vol. 57, pp. 678-683 (1985).

[5] J. Durnin, J. J. Miceli, and J. H. Eberly, "Diffraction-free beams," Phys. Rev. Lett., Vol. 58, pp. 1499-1501 (1987).

[6] I.M.Besieris, A.M.Shaarawi and R.W.Ziolkowski, "A bi-directional traveling plane wave representation of exact solutions of the scalar wave equation," J. Math. Phys., Vol.30, pp.1254-1269 (1989).

[7] J.-y. Lu and J. F. Greenleaf, "Experimental verification of nondiffracting X-waves," IEEE Trans. Ultrason. Ferroelectr. Freq. Control, Vol.39, 441-446 (1992).

[8] R.Donnelly and R.W.Ziolkowski, "Designing Localized Waves," Proc. Roy. Soc. London, A, Vol.440, pp.541-565 (1993).

[9] H. E. Hernandez-Figueroa, Michel Zamboni-Rached and E. Recami (editors), *Localized Waves*, 1st ed. Hoboken, USA: John Wiley & Sons, 2008.

[10] H.E. Hernandez Figueroa ; E. Recami and Michel Zamboni-Rached (editors), *Non-Diffracting Waves*, 1st ed. Weinheim: Wiley-VCH Verlag, 2014.

[11] I.M.Besieris, M.Abdel-Rahman, A.Shaarawi and A.Chatzipetros, "Two fundamental representations of localized pulse solutions of the scalar wave equation," Progress in Electromagnetic Research (PIER), Vol.19, pp.1-48 (1998).

[12] M.Zamboni-Rached, E.Recami and H.E.Hernández-Figueroa, "New localized Superluminal solutions to the wave equations with finite total energies and arbitrary frequencies," European Physical Journal D, Vol.21, pp.217-228 (2002).

[13] Michel Zamboni-Rached, "Unidirectional decomposition method for obtaining exact localized wave solutions totally free of backward components," Phys. Rev. A Vol. 79, 013816 (2009).

[14] A.M.Shaarawi, I.M.Besieris and T.M.Said, "Temporal focusing by use of composite X-waves", J. Opt. Soc. Am. A, Vol.20, pp.1658-1665 (2003).

[15] A.M.Shaarawi and I.M.Besieris, "Focusing of Ultra-Wideband Composite X Waves," in Ultra-Wideband, Short-Pulse Electromagnetics 6, edited by E. L. Mokole, M. Kragalott and K. R. Gerlach (Kluwer Academic Plenum Publishers, 2003). pp. 193-202.

[16] Michel Zamboni-Rached, A. Shaarawi, and E. Recami,"Focused X-shaped pulses," J. Opt. Soc. Am. A, Vol. 21, 1564-1574 (2004).

[17] L. Mackinnon: "A nondispersive de Broglie wave packet," Found. Phys., Vol. 8, pp.157 (1978).

[18] J.Salo and M.M.Salomaa: "Subsonic nondiffracting waves", Acoustics Res. Lett. Online, Vol. 2, pp. 31-36 (2001).

[19] P.Saari and K.Reivelt: "Generation and classification of localized waves by Lorentz transformations in Fourier space," Phys. Rev. E, Vol. 69 (2004).

[20] M. Zamboni-Rached and E. Recami, "Subluminal wave bullets: Exact Localized subluminal Solutions to the Wave Equations," Physical Review. A , Vol. 77, 033824 (2008).

[21] M.Zamboni-Rached: "Localized solutions: Structure and Applications," M.Sc. thesis (Phys. Dept., Campinas State University, 1999).

[22] M.Zamboni-Rached, "Localized waves in diffractive/dispersive media," PhD Thesis, Aug.2004, Universidade Estadual de Campinas, DMO/FEEC.

[23] R.W.Ziolkowski, I.M.Besieris and A.M.Shaarawi, "Aperture realizations of exact solutions to homogeneous wave-equations," J. Opt. Soc. Am. A, Vol.10, pp.75-87 (1993).

[24] Michel Zamboni-Rached, "Analytical expressions for the longitudinal evolution of nondiffracting pulses truncated by finite apertures," J. Opt. Soc. Am. A, Vol. 23, pp. 2166-2176 (2006)

[25] Michel Zamboni-Rached, Erasmo Recami, and Massimo Balma, "Simple and effective method for the analytic description of important optical beams when truncated by finite apertures," Appl. Opt., Vol. 51, pp. 3370-3379 (2012)

[26] M.Zamboni-Rached, "Stationary optical wave fields with arbitrary longitudinal shape by superposing equal frequency Bessel beams: Frozen Waves," Opt. Express, Vol.12, pp.4001-4006 (2004).

[27] M.Zamboni-Rached, "Diffraction-Attenuation resistant beams in absorbing media," Opt. Express, Vol. 14, pp.1804-1809 (2006).

[28] Tárcio A. Vieira, Marcos R. R. Gesualdi and Michel Zamboni-Rached, "Frozen waves: experimental generation," Optics Letters, Vol. 37, pp. 2034, (2012).

[29] Tárcio A. Vieira, Michel Zamboni-Rached and Marcos R. R. Gesualdi, "Modeling the spatial shape of nondiffracting beams: Experimental generation of Frozen Waves via holographic method," Opt. Commun., Vol. 315, pp. 374-380 (2014).

[30] J.L.Prego, M.Zamboni-Rached, E.Recami, and H.E.Hernandez-Figueroa, "Producing acoustic Frozen Waves: Simulated experiments", IEEE Trans. Ultrason. Ferroel. Freq. Control, Vol. 60, pp. 2414-2425 (2013).

[31] J. L. Prego-Borgesa, Michel Zamboni-Rached, Erasmo Recami and Eduardo Tavares Costa, "Producing acoustic Frozen Waves: Simulated experiments with diffraction/attenuation resistant beams in lossy media," Ultrasonics, Vol. 54, pp.1620-1630 (2014).